Comparative Study of the Surface Nanostructure Formation on Different Surfaces Generated by Low Number of fs Laser Pulses

Miklós FÜLE[*1], Anett GÁRDIÁN[2], Judit BUDAI[2] and Zsolt TÓTH[2,3]

[*1] *High Intensity Laser Laboratory, Department of Experimental Physics, University of Szeged, H-6720 Szeged, Dóm tér 9., Hungary*

E-mail: miklos.fule@gmail.com

[2] *Department of Optics and Quantum Electronics, University of Szeged, H-6720 Szeged, Dóm tér 9., Hungary*

[3] *Department of Oral Biology and Experimental Dental Research, University of Szeged, H-6720 Szeged, Tisza Lajos krt. 64, Hungary*

Despite the early observation of laser induced periodic surface structures, the mechanism responsible for their formation is still in the focus of an intense debate. To deduce the processes dominating the formation, we investigated the surface structuring of Si, GaAs and V surfaces by femtosecond laser pulses in identical conditions. All material surfaces showed the traces of melting at low pulse numbers, and in all cases ripples were observed with periods of several hundreds of nanometers. The orientation of the ripples appearing already in case of the smallest pulse number was perpendicular to the polarization of laser light. In case of Si, a second stripe system developed on the surface at higher pulse number. The orientation of this structure was parallel to the polarization of laser light, and had a period similar to the original stripe system. The formation of the observed structure is discussed in the frame of capillary waves excited by laterally periodic fluence and melting. The periodic excitation is attributed to the interference of the incoming and scattered laser light.

DOI: 10.2961/jlmn.2015.01.0014

Keywords: LIPSS, femtosecond laser pulses, pulse number dependence, capillary waves

1. Introduction

Surface modification is in the frontline of material researcher's projects due to the application possibilities in different kinds of research and industry projects. Besides chemical processes [1,2,3] the laser based surface modification processes provide controllable environment for the construction of a surface structure on base materials with planned properties [3]. The main benefit of these laser based techniques contrary to the chemical process based technologies is the capability to modify the surface without using any kind of poisoning lye or acid materials. In this way, it can be the base method for environment friendly technology processes.

Many publications deal with the different kinds of surface structures resulting from the interaction between different kinds of laser pulses with substrate materials [4-15]. The applied laser parameters (e.g. pulse length, wavelength, repetition rate, number of applied pulses) can be varied in wide range like other parameters of ambient (pressure, chemical composition). Among the numerous laser parameters the laser pulse duration and the laser wavelength are two main laser parameters during these processes that mainly determine the properties of the given nanostructures. One of the interesting nanostructures are the periodic ripples that can be observed after the irradiation of surface using ns [14], ps [12] and fs [5] pulses as well. Even though lot of studies deal with laser-induced periodic surface structures (LIPSS), the explanation of the formation of these periodic nanostructures is a more challenging task than the production of them. Several parallel theories try to explain the processes responsible for the surface structure evolution. To be able to deduce, which process is the dominant during the laser structuring of surfaces, as much as possible experimental details should be collected. Therefore, in this work we aimed to reveal the evolution of the nanostructure formation with increasing number of laser pulses on metal and semiconductor surfaces at exactly the same laser fluence, below the ablation threshold.

2. Experiments

In our experiments, a Ti:sapphire laser (central wavelength: 800 nm and pulse length: 30 fs) was used. The

energy at the sample surface was kept at 440 μJ and the energy density on the surfaces was 1 J/cm^2, if not stated otherwise in the text. The repetition rate of the laser pulses was 200 Hz. The laser beam was linearly polarized. Before the irradiation of the (100) silicon, the (111) GaAs wafers and mechanically polished vanadium pieces were cleaned in ultrasonic bath under acetone and ethanol separately. The beam of Ti:sapphire laser was directed by a dielectric mirror onto the sample surface perpendicularly and it was projected by a 60 mm focal length lens. The surface treatment was investigated at room temperature.

To examine the pulse number dependence, a shutter was used to control the pulse number between 3 and 1000. The spot size and thus the fluence of the certain sample position were estimated by determining the area of irradiated spots from beam profile measurements by knife edge method [16].

For the investigation of the modified surfaces, we used the high resolution scanning electron microscopy (SEM) mode of a Hitachi S-4700 microscope. The x axis of the presented electron microscope images is set parallel to the polarization direction. For further analysis Raman spectroscopy was perfomed by using a Thermo Scientific DXR Raman Microscope. The analysis of the SEM images was performed by ImageJ software.

3. Results

In the followings, we present the surface structures generated by different numbers of laser pulses. These structures were investigated with the help of SEM images, which can be seen on Figs. 1 - 4. in case of vanadium, silicon and gallium arsenide. The figures also contain the Fourier spectrum of the given SEM images in the bottom row. The SEM pictures cover 25x25 μm surfaces while the FFT images cover spatial frequency range of -10 to 10 cm^{-1} in both directions.

3.1 Vanadium surface

The scanning electron microscopy images about the treated vanadium surface area can be seen in Fig. 1. The evolution of the given structure can be followed parallel on the SEM images and their frequency spectrum. The surface texturization started from the lowest number of laser pulses (Fig. 1 a1)), where periodic ripples can be seen, which partly cover the treated surfaces. Despite the partial cover, the periodic feature can be detected on the FFT spectrum in the form of two bright areas on the two sides of the zero order (Fig. 1 a2)). As the pulse number is getting higher, the coverage and the periodicity of the texture became more obvious. In parallel, the bright areas become spots in the FFT spectrum, and get sharper. Above 50 laser shots a second pair of spots appear on the FFT spectra while the SEM images show more regular periodic structures.Finally the second spot pair disappears in case of 1000 laser shots. In cases of all pulse numbers, the orientation of the periodic structure is strictly perpendicular to the laser polarization direction.

3.2 Silicon surface

The evolution of the generated surface structure on silicon surface is presented in Fig. 2. In the case of low pulse numbers, the main form of the surface structure are randomly placed droplet like particles. The periodicity of the generated structure is not as obvious as in case on the vanadium surface at 3 laser shots however the FFT spectrum shows the signs of periodic feature, in the form of small bright spots. With the rising of laser pulse number, the coverage of the surface texture becomes denser, while the periodicity of this structure became more evident. Furthermore, at large shot numbers, a new type of structure appears with larger characteristic size: cracks are present on the surface and a smaller scale structure appears between these cracks. In case of 1000 laser pulses deep canyons cover the surface. Furthermore as pulse number reaches the value of 200, a second stripe system develops, which has a periodicity similar to the original stripe system and which is perpendicular to the original ripples according to the FFT spectrum. This second stripe system is more pronounced when lower fluence values are used for irradiation as shown in Fig 3. Actually the original stripe system vanishes in case of the 1000 pulse treatment, and besides the ripples being parallel to the laser polarization, a third stripe system can be seen on the edges of the deep cracks, that are at an angle of 35 degree from the polarization direction.

3.3 Gallium-arsenide surface

The third surface, where the structure evolution was followed, was the gallium-arsenide (110) surface. The SEM images of the generated nanostructures and the appropriate FFT spectrum can be seen in Fig. 4. In this case, the ripple formation also starts from the lowest applied laser pulse number: a periodic stripe system develops in case of the 3 laser shots treated surfaces, which is covered by the droplet like forms. Again, the periodic structure appears perpendicularly to the laser polarization direction. From the 50 laser pulses, a new type of surface texture arrangement appears and dominates the surface. The characteristic size of this new texture is much larger than the previously shown periodic structure and the size increases with pulse number. The small scale structure can be detected however on the large scale structures (see Fig. 4 e1) and the periphery of the laser treated areas.

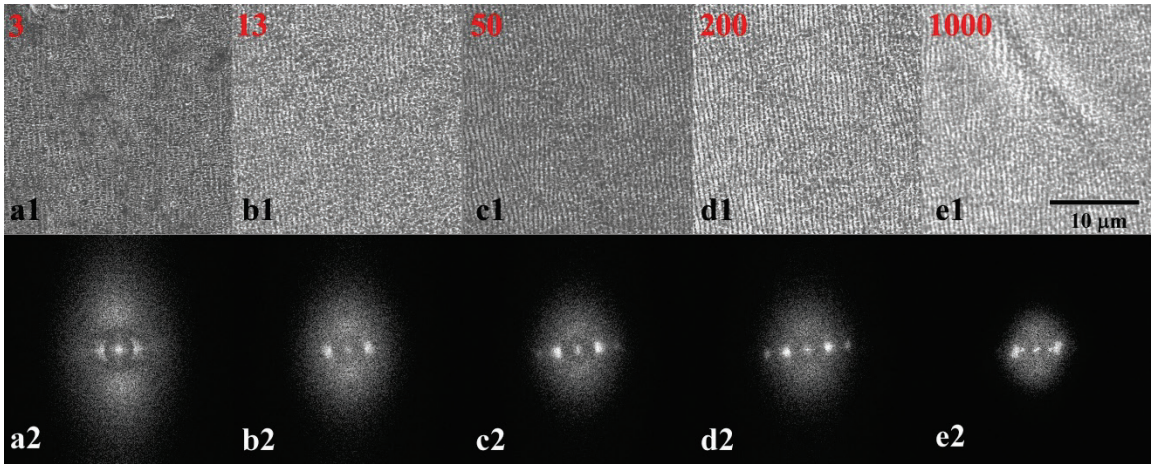

Figure 1. Scanning electron microscopy images from the modified Vanadium surfaces at 1 J/cm^2 laser fluence and their FFT spectra.

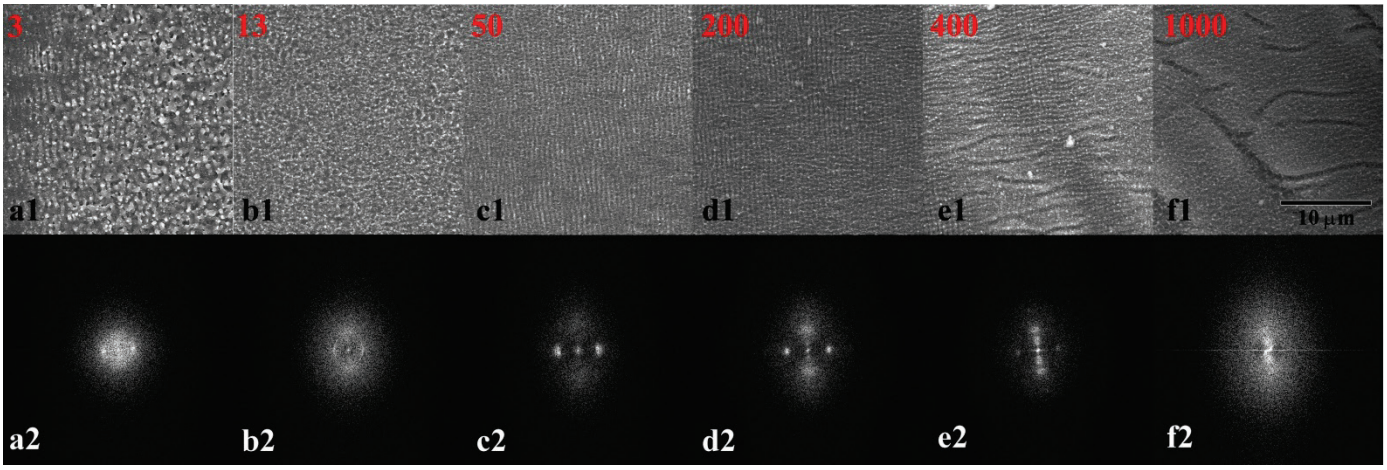

Figure 2. Scanning electron microscopy images from the modified silicon surfaces at 1 J/cm^2 laser fluence and their FFT spectra.

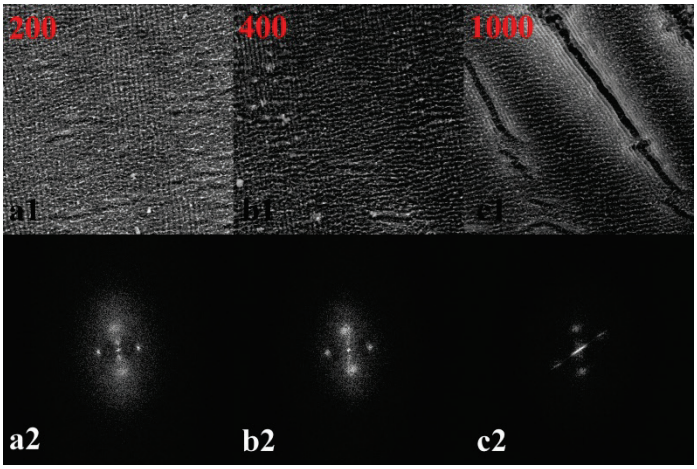

Figure 3. Scanning electron microscopy images from the modified silicon surface at 0.9 J/cm^2 laser fluence and their FFT spectra.

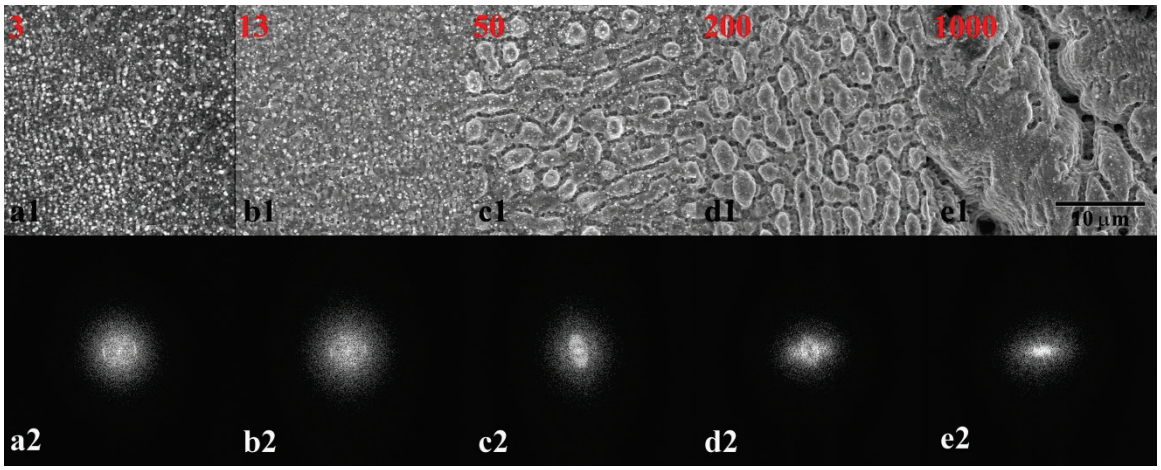

Figure 4. Scanning electron microscopy images from the modified gallium arsenide surfaces at 1 J/cm^2 laser fluence and their FFT spectra.

3.4 Structure evolution with pulse number

Finally we can describe the structure evolution of the generated periodic surface as a function of the applied laser pulses. From the calculated FFT spectra, the average periodicity of the structure was determined. For this purpose, the 512 pixel × 512 pixel images were cropped from the original images and the corresponding FFT images were calculated. Line sections from the FFT images along the detectable spectral features were used to read the periods of the features. This periodicity as a function of the applied laser pulses is presented in Fig. 5.

The periodicity of the produced structure is always smaller than the laser wavelength. In case of vanadium, the ripple width decreases from 680 nm to 560 nm continuously. In case of silicon, the ripple width is around the wavelength at 10 pulses but after that decreases drastically to 630 nm at 50 pulses. Finally the ripple width decreases to 580 nm at 1000 laser pulses. For the stripe system appearing above 200 pulses the ripple width is varying within measurement error around 550 nm for both presented fluence values. In case of GaAs samples, data is only presented up to 50 shots, since ripple width was not calculated when the larger size structure became dominant. However, in case of these low number of laser pulses, the line width also shows decreasing feature from 750 nm to 670 nm.

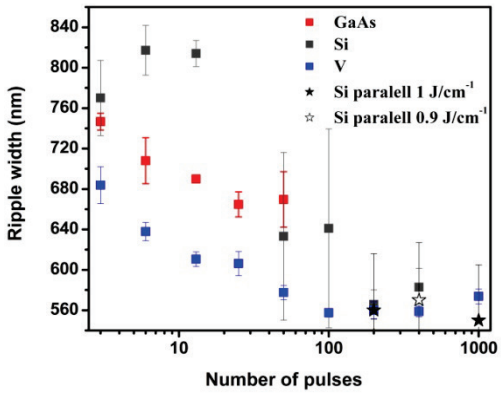

Figure 5. The ripple width of the periodic structure plotted as a function of the laser pulse number. Red, black and blue squares denote the width of ripples perpendicular to the polarization direction observed on GaAs, Si and V, respectively. Full and open stars denote the width of ripples parallel with the polarization direction observed on Si in case of 1 and 0.9 J/cm^2 fluence values, respectively.

3.5 Raman spectroscopy

To reveal the change in the composition of the laser treated surface, their bonding nature was analyzed by Raman spectroscopy. The resulting spectrum can be seen in Figs. 6 a-c. The black curve corresponds to the spectrum of intact surface in all cases while the green and red spectra correspond to the treated surfaces by 3 and 1000 laser shots, respectively.

In Fig. 6 a), the Raman spectra of the intact and treated surfaces of vanadium are presented. In the spectrum of intact surface, many Raman bands are present that can be identified as the active component of a-V_2O_5 structure (300 cm^{-1}, 487 cm^{-1}, 534 cm^{-1}, 790 cm^{-1}, 998 cm^{-1}) [17, 18]. The other components also belong to the different kinds of

V_xO_y structure's Raman active vibrational transitions (V_2O_2: 170 cm^{-1}, V=O: 270 & 866 cm^{-1})[18, 19]. After the surface treatment, the structure of the Raman spectrum completely changed. The bands described as the V_2O_5 completely vanishes while the intensity of the other bands are also decreased in the spectrum.

In Fig. 5 b), the Raman spectra of the treated and intact surfaces of silicon can be seen. The main difference between these spectra is the widening of the main band at 520 cm^{-1} belonging to crystalline Si [20]. This behavior of the spectrum shows the appearance of amorphization in the structure.

Finally in Fig 5 c), the Raman spectra of the intact and treated surfaces of the gallium arsenide are presented. The spectrum is drastically changed due to the treatment of different numbers of laser pulses. However, the main change occurs already after treatment by 3 laser pulses. The Raman active band at 298 cm^{-1} present in the spectrum of intact surface and corresponding to LO phonon in GaAs [21] is drastically weakened. Meanwhile, a narrow band appears around 240 cm^{-1} and a wider band in the range of 200 - 250 cm^{-1} is emerging, which could be the result of the segregation of Ga and As, since metallic Ga has a Raman band at 246 cm^{-1} [22] and the wide band was identified in [23] as the Raman band of amorphous As.

4. Discussion

LIPSS formation was observed for all cases, with ripple periods of several hundreds of nanometers for all investigated materials (Si, V, GaAs). Ripplewidth decreases with pulse number. At large pulse numbers, greaterstructuresalso appear (especially in case ofGaAs), however smaller scale ripples emerged on certain large scale objects. Formation of a structureperpendicular to the original direction of the ripples was detected in case of Si.

Many theories address the explanation of LIPSS formation. These are including the interference of the incoming and defect scattered light [9, 14], the interference effects with surface plasmon-polariton waves [6-8, 10, 11], hydrodynamic instabilities in the melt layer [4], self organized structure formation [5, 13] in the irradiating laser softened and perturbed target lattice, and most recently the combination of surface plasmon-polaritons and capillary waves in the melted material [24].

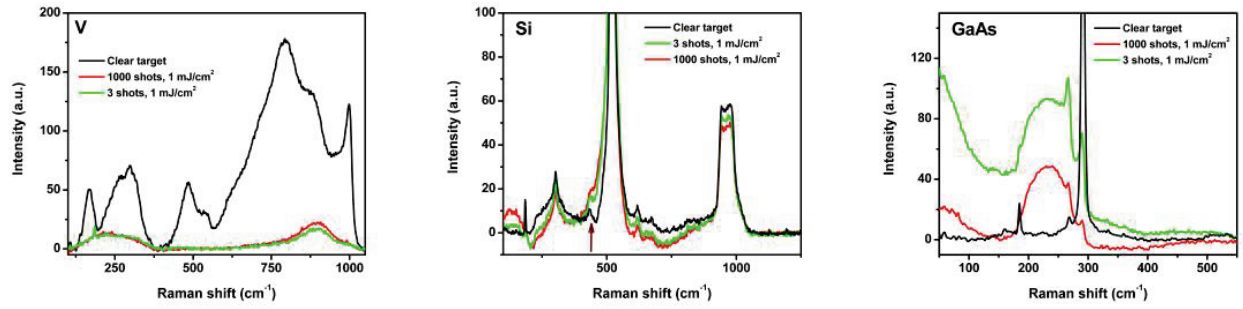

a, b, c,

Figure 6. Raman spectra of the intact and treated zones of a) vanadium, b) silicon and c) gallium arsenide surfaces.

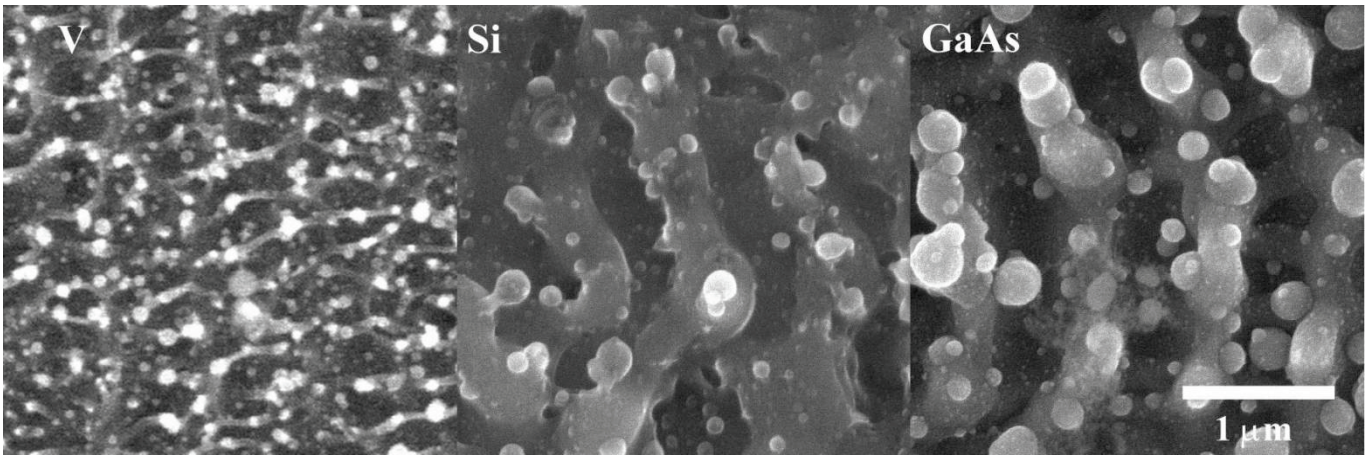

Figure 7. A SEM images from 3 μm x 3 μm V, Si and GaAs surfaces, shot by 3 Ti:sapphire laser pulses.

Higher magnification SEM images support that melting and local movement of molten phase occur during the formation of the ripples. Fig. 7 shows V, Si and GaAs surfaces after 3 laser shots. Formation of droplets and rims around molten areas can be clearly seen. Although the structures are rather different for the three materials, the periodicity of the darker holes are rather close to the length of the periodicity of the structures that is determined in the experimental part. Furthermore, the vertical alignment of the dark areas (holes) can be seen. The appearance of frozen rims support that the formation of the ripples can be connected in all three cases to hydrodynamical processes present in the melted region, which can enable the formation of capillary waves.

The period of the small scale ripple structure falls in the order of the wavelength of the incoming laser light. This is most pronounced in case of the Si surface, where the period of the lowest pulse numbers is 780-810 nm. This observation and the orientation of the ripples suggest that the formation process is initiated by the interference of the laser light, since the direction of the ripples are determined by the direction of the polarization. This fact supports the model, when the light reflected from defects, present or created by previous intense laser pulses, interferes with the incoming light. Interference is the strongest and becomes dominant to that direction, where the reflected intensity from a surface structure (e.g. a droplet) is maximal. As described in [14], the reflectivity is higher in the incident plane, which is perpendicular to the direction of polarization of the incoming light. The interference pattern determines the structure: at locations of instructive interference the local fluence is higher than at positions where destructive interference appears, therefore the excitation of the material is more effective. The period of the structure in case of normal incidence is: $L = \lambda/n$, where n is the refractive index of the modified layer of the material. The periodicity of the ripples at low pulse numbers correspond to refractive indices of 1 for Si, 1.2 for V and 1.07 for GaAs. As the pulse number increases, the decrease in the ripple width suggest the increase of the refractive index to 1.4 for all substrates. The initial values are much smaller than the bulk refractive indices of the substrates, and indicate that the interference occurs in air, above the sample surface. As the pulse number increases the decrease in the ripple width suggest the increase of the refractive index to 1.4 for all substrates. This observed pulse number dependence can be explained in the frame of the interference model, supposing the modification of the top layer of the surface. The increase of the surface roughness increases the effective refractive index of the surface region according to Effective Medium Approximation [25]. Furthermore i) in case of Si amorphization is observed, which lowers the refractive index of the top layer, and earlier studies showed that the surface is oxidized [26], ii) the development of a surface oxide which has again lower refractive indices is detected for the V samples. The composition of GaAs is noticed to be changed. Despite the deficiencies of the interference model the strong dependence of the ripple orientation on the polarization state of the laser suggest that, the instabilities within the melted layer are not formed randomly but are strongly influenced by the interference phenomena.

Therefore, the following scenario can be plotted based on our experimental results. The material, namely the electron system, is excited periodically due to the interference of the incoming and scattered wave. This excitation results in the melting and evaporation of the surface when the electron system transfers the energy to the lattice much after the laser pulse on a ps time scale [27]. After evaporation of the surface, a molten layer remains on the surface which preserves the traces of the periodic excitation in the form of domains of higher temperatures and pressures causing the formation of thermal instabilities or capillary waves. Capillary waves might be reflected from the periphery of the laser treated area, or from the developing larger scale structures and the wavefront of the reflected waves will close an angle with the original wavefronts. Finally, during the resolidification of the surface the instantaneous morphology is preserved in the form of LIPSS. Similar description was developed in [24], where the origin of the instabilities was connected to the generation of surface plasmons, and the decrease of the ripple width with the pulse number was completely described on hydrodinamical base. The discovery of the motion of capillary waves during or after the laser excitation would certainly help to move from speculative explanations to appropriate theory. An inverse experiment to our presented methods, i.e. detection of the corresponding diffraction patterns would serve with valuable information about LIPSS formation. Carefully designed pump and probe experiments are capable to record ultrafast movements, which initiated by fs laser pulses [28]. Through the study of the evolution of diffraction patterns in ps scale a more insight could be gained to understand the dynamics of these processes.

The origin of the some micrometer range structures can be explained by the texture decreased reflectivity. As the surface of the sample becomes structured scattering of the surface is increased, therefore the direct reflection is decreased. However, the amount of light coupled into the sample can be increased due to multiple reflections within the valleys of the structures. These would increase the local fluence at deeper points. If the threshold fluence of ablation is exceeded, further deepening of the valleys take place, due to the onset of ablation.

5. Conclusions

We have shown that LIPSS formation observed for the irradiation of Si, V and GaAs surfaces with fs lasers takes place in a melted layer according to the droplets present in high magnification SEM images of the surface. This suggests that capillary waves and hydrodynamical effects take place during ripple formation. This suggestion is further supported by the observation that two, mutually perpendicular ripple systems develop on the surface of Si. Finally we have discussed that the orientation of the ripples

significantly depends on the polarization of laser light suggesting that the formation is initiated by the interference effect, causing periodic energy distribution during the excitation of material.

Acknowledgements

The project was partially funded by TÁMOP-4.2.2.A-11/1/KONV-2012-0047– "New functional materials and their biological and environmental answers" and is supported by the European Union and co-financed by the European Social Fund.

References

[1] I. Cook, D. W. Sheel, J. L. Hodgkinson: Surface & Coatings Technology 205 (2011) S567–S572;

[2] L.M. Apátiga , E. Rubio, E. Rivera a , V.M. Castaño: Surface & Coatings Technology 201 (2006) 4136 – 4138;

[3]J. Yang et al., Light: Science & Applications 3, e185 (2014)

[4] E.L. Gurevich: Appl. Surf. Sci. 278 (2013) 52–56

[5] O. Varlamova, M. Bounhalli, J. Reif: Appl. Surf. Sci. 278 (2013) 62–66

[6]J. Bonse, A. Rosenfeld, J. Krüger: J. Appl. Phys. 106, (2009) 104910

[7]J. Bonse, J. Krüger: J. Appl. Phys. 108, (2010) 034903

[8]T. J.-Y. Derrien, T. E. Itina, R. Torres, T. Sarnet, M. Sentis: J. Appl. Phys. 114, (2013) 083104

[9]R. L. Harzic, D. Dörr, D. Sauer, M. Neumeier, M. Epple, H. Zimmermann, F. Stracke: Optics Lett. vol. 36, no. 2 (2011) 229-231

[10]M. Huang, F. Zhao, Y. Cheng, N. Xu, Z. Xu: Optics Express vol. 18, no. S4 (2010) A600-619

[11]F. Garrelie, J. P. Colombier, F. Pigeon, S. Tonchev, N. Faure, M. Bounhalli, S. Reynaud, O. Parriaux: Optics Express vol. 19, no. 10 (2011) 9035-9043

[12] M. Schüle, M. Afshar, D. Feili, H. Seidel, K. König, M. Straub: Appl. Surf. Sci. vol. 314, (2014) 21-29

[13] J. Reif, O. Varlamova, S. Varlamov, M. Bestehorn: Appl. Phys. A (2011) 104:969–973 J16

[14] M. Csete, Zs. Bor, Applied Surface Science 133 (1998) 5–16

[15] K. Sokolowski-Tinten and D. von der Linde: Phys. Rev. B vol. 61, no. 4 (2000) 2643-2650

[16] Y. Suzaki, A. Tachibana: Appl. Optics, vol. 14, no. 12 (1975) 2809-2810

[17] S. H. Lee, H. M. Cheong, M. J. Seong, P. Liu, C. E. Tracy, A. Mascharenhas, J. R. Pitts, S. K. Deb: J. Appl. Phys. Vol. 92, no. 4, (2002) 1893-1897

[18] B. Zhou, D. He: J. Raman Spectrosc, 39 (2008) 1475–1481

[19] W. Chen, Ã. L. Mai, J. Peng, Q. Xu, Q. Zhu: J. Solid State Chemistry 177 (2004) 377–379

[20] P. P. Dey, A. Khare: Appl. Surf. Sci. vol. 307 (2014) 77-85

[21] Porous III-V Semiconductors: online book: www.porous-35.com

[22] J.A. Creighton, R. Withnall: Chemical Physics Letters, vol. 326, Iss. 3–4 (2000) 311–313

[23] D. S. Jiang, X.-P. Li, B.-Q. Sun, H.-X. Han: Phys. D: Appl. Phys. 32 (1999) 629–631

[24] G. D. Tsibidis, M. Barberoglou, P. A. Loukakos, E. Stratakis, and C. Fotakis: Phys. Rev. B 86 (2012) 115316

[25] C. Liu, L. Panetta, P. Yang: Journal of Quantitative Spectroscopy & Radiative Transfer 146 (2014) 331–348

[26] Z. Toth, I. Hanyecz, A. Gárdián, J. Budai, J. Csontos, Z. Pápa, M. Füle: Thin Solid Films, In Press, Corrected Proof, Available online 28 October 2013

[27] E. Gamaly: Femtosecond Laser-Matter Interactions, Pan Stanford Publihing Pte. Ltd (2011)

[28] Z. Toth, B. Hopp, J. Klebniczki, N. Kresz, Z. Bor, D. Anglos, C. Kalpouzos, C. Fotakis, Appl. Phys. A 79 (2004) 1287-1290

(Received: July 18, 2014, Accepted: December 23, 2014)